Supporting Information

Exploration of Alternative Scaffolds for $P2Y_{14}$ Receptor Antagonists Containing a Biaryl Core

Young-Hwan Jung,[†^] Jinha Yu,[†^] Zhiwei Wen,[†] Veronica Salmaso,[†] Tadeusz Karcz,[+] Ngan B. Phung,[†] Zhoumou Chen,[¥] Sierra Duca,[†] John M. Bennett,[†] Steven Dudas,[†] Daniela Salvemini,[¥] Zhan-Guo Gao,[†] Donald N. Cook,[+] and Kenneth A. Jacobson[†*]

[†] Molecular Recognition Section, Laboratory of Bioorganic Chemistry, National Institute of Diabetes and Digestive and Kidney Diseases, National Institutes of Health, Bethesda, MD 20892 USA.

[+] Immunity, Inflammation and Disease Laboratory, National Institute of Environmental Health Sciences, National Institutes of Health, Research Triangle Park, NC 27709 USA.

[¥] Department of Pharmacology and Physiology and the Henry and Amelia Nasrallah Center for Neuroscience, Saint Louis University School of Medicine, 1402 South Grand Blvd., St. Louis, MO 63104, USA.

Contents

Chemical Synthesis

Scheme S1. Synthesis of 4-bromophenyl intermediates for bicyclic piperidine substitutions of **1** and **2**.

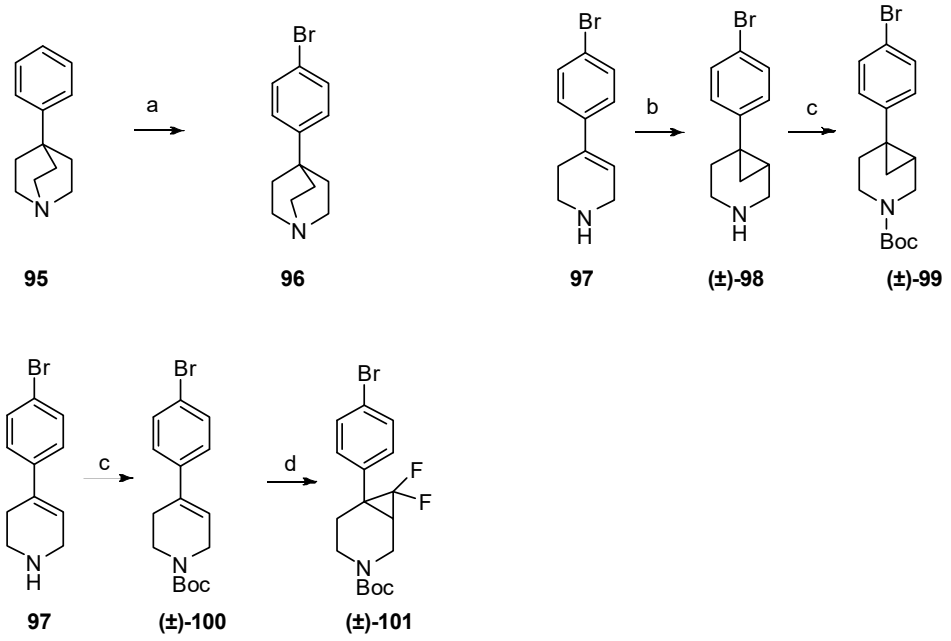

Reagents and Conditions: (a) AcOH, Br_2, reflux, 4.5 h, 72%; b) Et_2Zn, CH_2I_2, CH_2Cl_2, Ar, rt, overnight, 62%; (c) $(Boc)_2O$, TEA, DCM, 0 °C to rt, 2 h, 78-81%; (d) $TMSCF_3$, NaI, THF, 65°C, overnight, 16%.

Scheme S2. Carboxylate substitutions on the central phenyl ring of **2**.

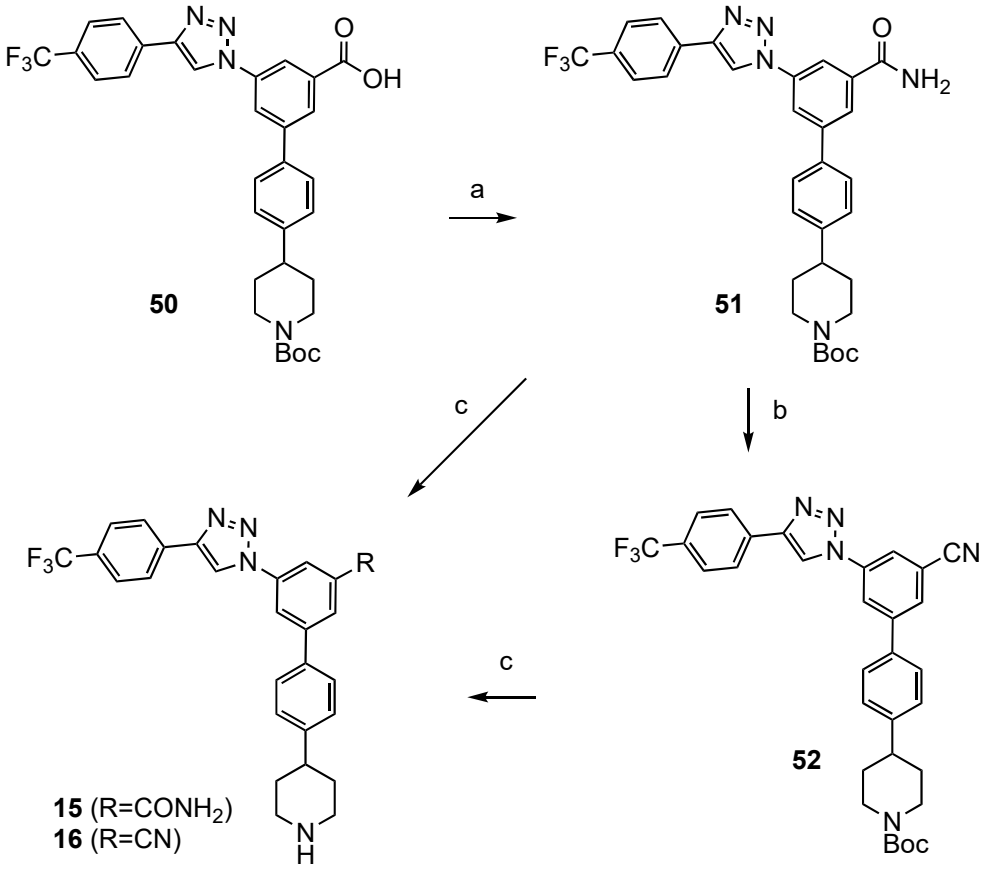

Reagents and Conditions: (a) NH_4Cl, HATU, DIPEA, DMF, rt, 1 h, 99%; (b) $(CF_3CO)_2O$, Et_3N, DCM, rt, 1 h, 76%; (c) TFA:THF = 2:1, rt, 0.5 h, 72% (**15**) or 87% (**16**).

Synthetic procedures

Preparation of $P2Y_{14}R$ antagonist intermediates for Suzuki coupling (Scheme S1)

4-(4-Bromophenyl)quinuclidine (**96**). Bromine (2 mL) was added to a stirred solution of 4-phenylquinuclidine **95** (375 mg, 2 mmol) in AcOH (35 mL). The mixture was refluxed in a 140 ºC oil bath for 4.5 h. The reaction residue was cooled to rt and basified with 6 N NaOH and extracted with CH_2Cl_2 three times. The combined organic layer was dried with Na_2SO_4. The volatiles were evaporated and the residue was column chromatographed (CH_2Cl_2/MeOH/TEA, 100:0:1→85:15:1) and further purified on RP-HPLC (t_R =23 min; C18; A: ACN, B: 0.2% TFA in H_2O; 30% A → 60% A in 40 min, flow rate = 5 mL/min) to give **96** as a white solid (384 mg, 72%): ^{1}H NMR (400 MHz, $CDCl_3$) δ 7.53 (d, *J* =8.3 Hz, 2H), 7.31 (d, *J* =8.2 Hz, 2H), 3.90 (t, *J* =7.4 Hz, 6H), 2.21 (t, *J* =7.2 Hz, 6H); HRMS m/z $[M+H]^+$ for $C_{13}H_{17}BrN$ calculated 266.0539, found 266.0541.

6-(4-Bromophenyl)-3-azabicyclo[4.1.0]heptane (**98**). A 25 mL round-bottom flask was flamed dried under argon and charged with 4-(4-bromophenyl)-1,2,3,6-tetrahydropyridine **97** (95.2 mg, 0.4 mmol) and CH_2Cl_2

(4 mL). Into the solution cooled in ice bath was added diethylzinc (1M in hexane, 1 mL, 1 mmol). The mixture was stirred at 0 ºC for 30 min and then diiodomethane (161.1 µL, 535.7 mg, 2 mmol) was added. The resulting mixture was stirred at 0 ºC for 1.5 h and then at rt overnight. The reaction was quenched with saturated NH_4Cl solution and then basified with $NaHCO_3$ solution and extracted with CH_2Cl_2 three times. The combined organic layer was dried with Na_2SO_4. The volatiles were evaporated and the residue was column chromatographed (CH_2Cl_2/MeOH/TEA, 100:0:1→95:5:1) to give **98** as transparent oil (62.8 mg, 62%): ^{1}H NMR (400 MHz, $CDCl_3$) δ 7.38 (d, *J* =8.1 Hz, 2H), 7.20 (d, *J* =8.1 Hz, 2H), 5.96 (s, 1H), 3.60-3.55 (m, 1H), 3.12 (d, *J* =13.2 Hz, 1H), 3.05-2.95 (m, 1H), 2.75-2.69 (m, 1H), 2.24-2.09 (m, 2H), 1.36-1.31 (m, 1H), 1.08-1.05 (m, 1H), 0.92 (t, *J* =5.3 Hz, 1H). HRMS m/z $[M+H]^+$ for $C_{12}H_{15}BrN$ calculated 252.0382, found 252.0387.

N-Boc-6-(4-bromophenyl)-3-azabicyclo[4.1.0]heptane (**99**). To a solution of **98** (62.8 mg, 0.25 mmol) in CH_2Cl_2 (2.5 mL) was added TEA (123 µL, 89 mg, 0.88 mmol) and $(Boc)_2O$ (71.2 mg, 0.33 mmol) at 0 ºC. The resulting solution was stirred at rt for 2 h. The reaction was quenched with $NaHCO_3$ solution and extracted with CH_2Cl_2 three times. The combined organic layer was dried with Na_2SO_4. The volatiles were evaporated and the residue was column chromatographed (hexane/EtOAc, 100:0→90:10) to give **99** as a white solid (68.5 mg, 78%): ^{1}H NMR (400 MHz, $CDCl_3$) δ 7.38 (d, *J* =8.4 Hz, 2H), 7.10 (d, *J* =8.4 Hz, 2H), 3.80-3.71 (m, 2H), 3.40-3.34 (m, 1H), 3.25-3.19 (m, 1H), 2.10-2.04 (m, 2H), 1.46 (s, 9H), 1.39-1.30 (m, 1H), 0.954 (dd, *J* =5.2, 8.9 Hz, 1H), 0.83 (t, *J* =5.3 Hz, 1H). MS m/z $[M-t\text{-butyl}+2H]^+$ for $C_{13}H_{15}BrNO_2$ calculated 296.0, found 296.0.

N-Boc-4-(4-bromophenyl)-1,2,3,6-tetrahydropyridine (**100**). To a solution of **97** (102.4 mg, 0.43 mmol) in CH_2Cl_2 (3 mL) was added TEA (212 µL, 153 mg, 1.5 mmol) and $(Boc)_2O$ (122 mg, 0.57 mmol) at 0 ºC. The resulting solution was stirred at rt for 2 h. The reaction was quenched with $NaHCO_3$ solution and extracted with CH_2Cl_2 three times. The combined organic layer was dried with Na_2SO_4. The volatiles were evaporated and the residue was column chromatographed (hexane/EtOAc, 100:0→90:10) to give **100** as a white solid (117 mg, 81%): ^{1}H NMR (400 MHz, $CDCl_3$) δ 7.42 (d, *J* =8.5 Hz, 2H), 7.21 (d, *J* =8.4 Hz, 2H), 6.01 ("s", 1H), 4.05 ("s", 2H), 3.62 (t, *J* =5.5 Hz, 2H), 2.47 ("s", 2H), 1.48 (s, 9H).

N-Boc-7,7-difluoro-6-(4-bromophenyl)-3-azabicyclo[4.1.0]heptane (**101**). To a solution of **100** (169 mg, 0.5 mmol) in THF (3 mL) in a pressure tube was added NaI (37.5 mg, 0.25 mmol) and $TMSCF_3$ (369 µl, 710 mg, 2.5 mmol). The reaction vessel was sealed and heated at 65 ºC overnight. The volatiles were evaporated and the residue was column chromatographed (hexane/EtOAc, 90:10→85:15) to give **101** as a white solid (31 mg, 16%): ^{1}H NMR (400 MHz, $CDCl_3$) δ 7.48 (d, *J* =8.3 Hz, 2H), 7.15 (d, *J* =8.3 Hz, 2H), 4.26-4.09 (m, 1H), 3.99-3.66 (m, 1H), 3.55-3.42 (m, 1H), 3.37-3.12 (m, 2H), 2.29-2.09 (m, 1H), 2.08-1.89 (m, 1H), 1.48 (s, 9H); ^{19}F NMR δ -129.2 (dd, *J* =90, 155.9 Hz, 1F), -145.2 (dd, *J* =149.6 Hz, 1F). HRMS m/z $[M-t\text{-butyl}+2H]^+$ for $C_{13}H_{13}BrF_2NO_2$ calculated 332.0092, found 332.0103.

Synthesis of compound 15-16 for carboxylate substitutions on the central phenyl ring of 2 (Scheme S2)

4'-(Piperidin-4-yl)-5-(4-(4-(trifluoromethyl)phenyl)-1*H*-1,2,3-triazol-1-yl)-[1,1'-biphenyl]-3-carboxamide (**15**). Method B: Yield 72%; HPLC purity 99% (R_t = 9.29 min); ^{1}H NMR (400 MHz, CD_3OD) δ 9.23 (s, 1H), 8.42 (s, 1H), 8.38 (s, 1H), 8.29 (s, 1H), 8.18 (d, *J* =8.12 Hz, 2H), 7.83-7.80 (m, 4H), 7.48 (d, *J* =8.20 Hz, 2H), 3.56 (d, *J* =12.80 Hz, 2H), 3.22-3.15 (m, 2H), 3.06-2.98 (m, 1H), 2.17-2.14 (m, 2H), 2.03-1.92

(m, 2H); MS (ESI, m/z) 492.2 $[M+1]^+$; ESI-HRMS calcd. m/z for $C_{27}H_{25}N_5OF_3$ 492.2011, found 492.2013 $[M+1]^+$.

4'-(Piperidin-4-yl)-5-(4-(4-(trifluoromethyl)phenyl)-1*H*-1,2,3-triazol-1-yl)-[1,1'-biphenyl]-3-carbonitrile (**16**). Method B: Yield 87%; ^{1}H NMR (400 MHz, CD_3OD) δ 9.28 (s, 1H), 8.55 (s, 1H), 8.36 (s, 1H), 8.19-8.17 (m, 3H), 7.83-7.82 (m, 4H), 7.50 (s, 1H), 7.49 (s, 1H), 3.55 (d, *J* =12.4 Hz, 2H), 3.24-3.16 (m, 2H), 3.07-3.01 (m, 1H), 2.15 (d, *J* =13.76 Hz, 2H), 2.03-1.93 (m, 2H); MS (ESI, m/z) 474.2 $[M+1]^+$; ESI-HRMS calcd. m/z for $C_{27}H_{23}N_5F_3$ 474.1906, found 474.1912 $[M+1]^+$.

tert-Butyl 4-(3'-carbamoyl-5'-(4-(4-(trifluoromethyl)phenyl)-1*H*-1,2,3-triazol-1-yl)-[1,1'-biphenyl]-4-yl)piperidine-1-carboxylate (**51**). To a solution of compound **50** (47 mg, 0.079 mmol; synthesized according to literature procedures reported) in dimethylformamide (3 mL) were added NH_4Cl (8.5 mg, 0.159 mmol), HATU (45 mg, 0.119 mmol) and *N*,*N*-diisopropylethylamine (20 mg, 28 µl, 0.159 mmol), and then this reaction mixture was stirred at room temperature for 1 h. This mixture was partitioned ethyl acetate (6 mL) and water (3 mL). The aqueous layer was extracted with ethyl acetate (5 mL x 2), and then the combined organic layer was washed with brine (3 mL), dried ($MgSO_4$), filtered and evaporated under reduced pressure. The residue was purified by silica gel column chromatography (hexane:ethyl acetate=1:1) to afford compound **51** (48 mg, 99%) as a white solid; ^{1}H NMR (400 MHz, $CDCl_3$) δ 8.44 (s, 1H), 8.27 (s, 1H), 8.23 (s, 1H), 8.11 (s, 1H), 8.07 (d, *J* =8.04 Hz, 2H), 7.76 (d, *J* =8.16 Hz, 2H), 7.66 (d, *J* =8.24 Hz, 2H), 7.38 (d, *J* =8.20 Hz, 2H), 4.31 (d, *J* =13.68 Hz, 2H), 2.89-2.81 (m, 2H), 2.80-2.73 (m, 1H), 1.89 (d, *J* =12.00 Hz, 2H), 1.67 (merged with water peak), 1.51 (s, 9H); MS (ESI, M/Z) 536.1 $[M+1\text{-}tert\text{-butyl}]^+$, 592.2 $[M+1]^+$; ESI-HRMS calcd. m/z for $C_{28}H_{25}N_5O_3F_3$ 536.1909, found 536.1911 $[M+1\text{-}tert\text{-butyl}]^+$.

tert-Butyl 4-(3'-cyano-5'-(4-(4-(trifluoromethyl)phenyl)-1*H*-1,2,3-triazol-1-yl)-[1,1'-biphenyl]-4-yl)piperidine-1-carboxylate (**52**). To a solution of compound **51** (41 mg, 0.069 mmol) in dichloromethane (2 mL) were added trifluoroacetic anhydride (97 mg, 64 µl, 0.462 mmol) and triethylamine (50 mg, 69 µl, 0.494 mmol) at 0 °C, and then this reaction mixture was stirred at room temperature for 1 h. This mixture was partitioned dichloromethane (6 mL) and water (3 mL). The aqueous layer was extracted with dichloromethane (5 mL x 2), and the organic layer was washed with brine (3 mL), dried ($MgSO_4$), filtered and evaporated under reduced pressure. The residue was purified by silica gel column chromatography (hexane:ethyl acetate=4:1) to afford compound **52** (30 mg, 76%) as a white solid; ^{1}H NMR (400 MHz, $CDCl_3$) δ 8.38 (s, 1H), 8.31 (t, *J* =1.84 Hz, 1H), 8.07 (d, *J* =8.08 Hz, 2H), 8.06-8.04 (m, 1H), 7.96 (t, *J* =1.42 Hz, 1H), 7.77 (d, *J* =8.20 Hz, 2H), 7.62 (d, *J* =8.28 Hz, 2H), 7.39 (d, *J* =8.20 Hz, 2H), 4.31 (d, *J* =12.84 Hz, 2H), 2.89-2.83 (m, 2H), 2.79-2.72 (m, 1H), 1.89 (d, *J* =12.04 Hz, 2H), 1.75-1.65 (m, 2H), 1.52 (s, 9H); MS (ESI, M/Z) 518.1 $[M+1\text{-}tert\text{-butyl}]^+$; ESI-HRMS calcd. m/z for $C_{28}H_{23}N_5O_2F_3$ 518.1804, found 518.1801 $[M+1\text{-}tert\text{-butyl}]^+$.

Figure S1. Structure of high affinity fluorescent tracer MRS4174 (36)

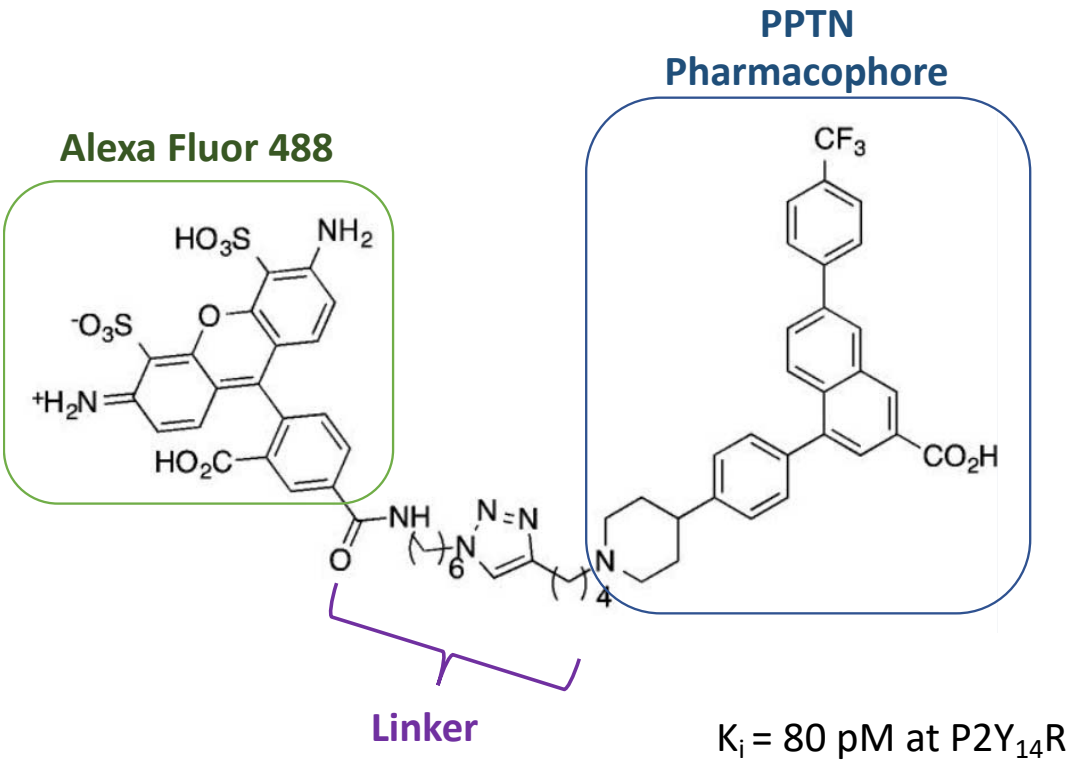

Off-target interactions:

Determined by the the Psychoactive Drug Screening Program (PDSP) at the University of North Carolina. We thank Dr. Bryan L. Roth (Univ. North Carolina at Chapel Hill) and National Institute of Mental Health's Psychoactive Drug Screening Program (Contract # HHSN-271-2008-00025-C) for screening data.

Reference: Besnard, J.; Ruda, G. F.; Setola, V.; Abecassis, K.; Rodriguiz, R. M.; Huang, X. P.; Norval, S.; Sassano, M. F.; Shin, A. I.; Webster, L. A.; Simeons, F. R.; Stojanovski, L.; Prat, A.; Seidah, N. G.; Constam, D. B.; Bickerton, G. R.; Read, K. D.; Wetsel, W. C.; Gilbert, I. H.; Roth, B. L.; Hopkins, A. L. Automated design of ligands to polypharmacological profiles. *Nature* **2012**, *492*, 215–220.

Procedures: https://pdsp.unc.edu/pdspweb/content/UNC-CH%20Protocol%20Book.pdf

Unless noted in the text, no significant interactions (<50% inhibition at 10 μM) for any of the nucleosides were found at the following sites (human unless noted): $5HT_{1A}$, $5HT_{1B}$, $5HT_{1D}$, $5HT_{1E}$, $5HT_{2A}$, $5HT_{2B}$, $5HT_{2C}$, $5HT_3$, $5HT_{5A}$, $5HT_6$, $5HT_7$, α_{1A}, α_{1B}, α_{1D}, α_{2A}, α_{2B}, α_{2C}, β_1, β_2, β_3, BZP rat brain site, D_1, D_2, D_3, D_4, D_5, delta opioid receptor (DOR), $GABA_A$, H_1, H_2, H_3, H_4, M_1, M_2, M_5, mu opioid receptor (MOR), σ_1, σ_2, DAT, NET, SERT. Representative curves are shown.

4, MRS4544, 53888; K_i value (μM): σ_2R, >6.2.
6b, MRS4574, 52187; none.
7a, MRS4149, 52188; none.
8, MRS4625, 55252; K_i values (μM): TSPO, 0.51; $5HT_{1D}$, 1.75; $5HT_{1E}$, 4.52; $5HT_{5A}$, 2.34; D_1, 1.39; D_5, 4.37; α_{1A}, 3.14; α_{1B}, 5.90; β_3, 0.86; DOR, 4.85. (reported in Mufti et al., 2020).[1]
12, MRS4571, 52189; K_i values (μM): KOR, 1.79; $5HT_{2A}$, 1.37; σ_1R, 0.66; σ_2R, 0.56.
17, MRS4608, 54182; K_i value (μM): 2.29 (σ_2R).
18, MRS4619, 54563; K_i values (μM): σ_2R, 1.35; $5HT_{1D}$, >8.9;
19, MRS4609, 54090; K_i values (μM): σ_2R, 0.30; DOR, 2.63.
21, MRS4616, 54562; K_i value (μM): σ_2R, 0.40.
22, MRS4478, 45539 K_i value (μM): 6.89 ($5HT_6$R). (reported in Yu et al., 2018).[2]
23, MRS4458, 45182; K_i values (μM): 3.26±0.64 (DOR), 4.34 ($5HT_{1D}$R). (reported in Yu et al., 2018).[2]
24, MRS4527, 50327; K_i values (μM): 2.48 (DOR), 0.50 (σ_1R), 2.91 (σ_2R).
25, MRS4525, 50325; K_i values (μM): 3.79 (DOR), 0.96 (α_{2A}R), 5.33 (α_{2B}R), 2.71±0.21 (α_{2C}R), 1.48 (σ_1R), 2.09 (σ_2R).
26, MRS4526, 50326; K_i values (μM): 2.96 (DOR), 1.11 (σ_1R).

1. Mufti, F.; Jung, Y. H.; Giancotti, L. A.; Yu, J.; Chen, Z.; Phung, N. B.; Jacobson, K. A.; Salvemini, D. $P2Y_{14}$ receptor antagonists reverse chronic neuropathic pain in a mouse model. *ACS Med. Chem. Lett.* **2020**, *11*, 1281−1286.
2. Yu, J.; Ciancetta, A.; Dudas, S.; Duca, S.; Lottermoser, J.; Jacobson, K. A. Structure-guided modification of heterocyclic antagonists of the $P2Y_{14}$ receptor. *J. Med. Chem.* **2018**, *61*, 4860−4882.

Figure S2.

σ_2 binding of **17** MRS4608 (PDSP 54182)

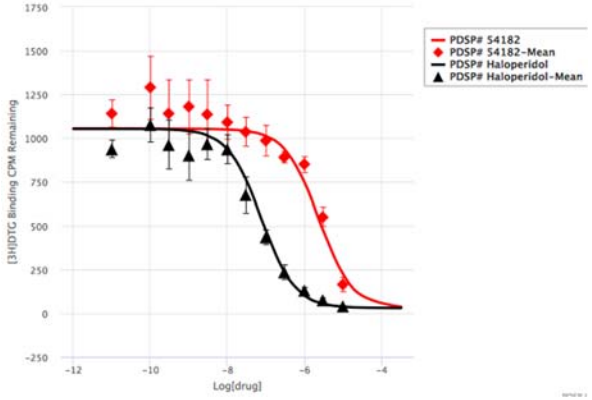

DOR binding of **19** MRS4609 (PDSP 54090)

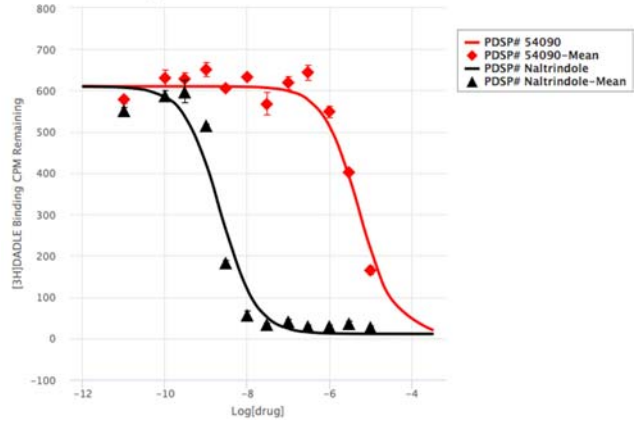

σ_2 binding of **19** MRS4609 (PDSP 54090)

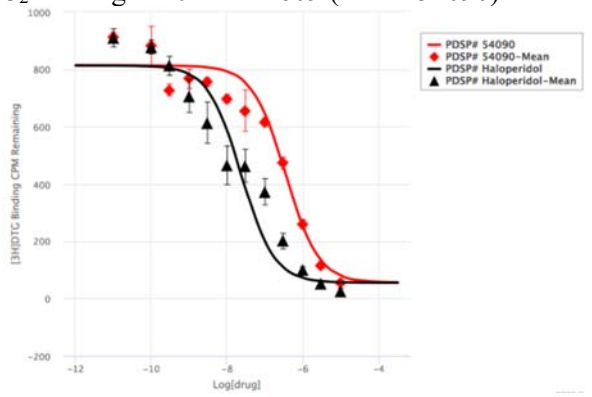

α_{2A} binding of **25** MRS4525 (PDSP 50325)

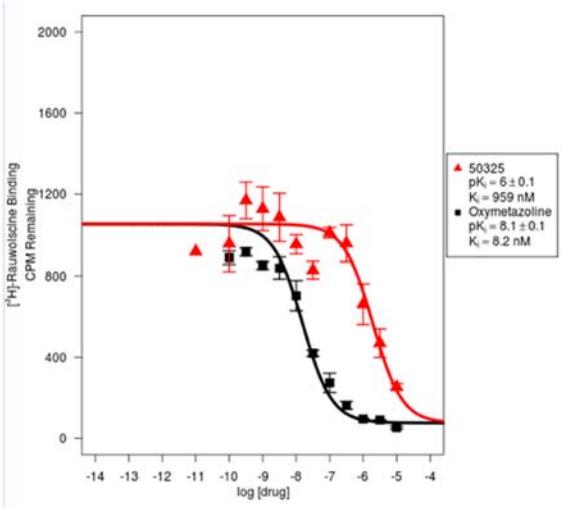

α_{2B} binding of **25** MRS4525 (PDSP 50325)

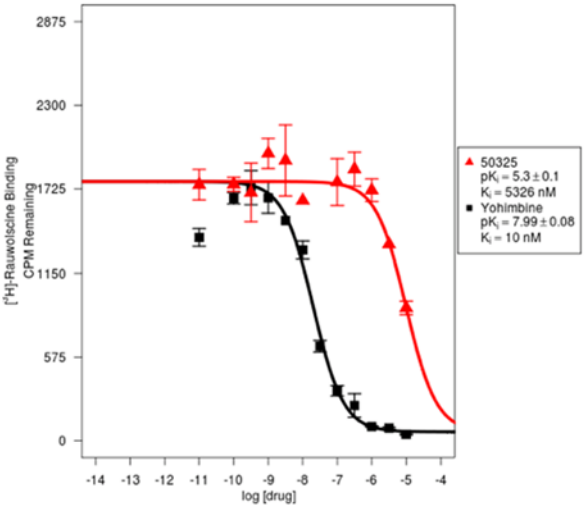

α_{2C} binding of **25** MRS4525 (PDSP 50325)

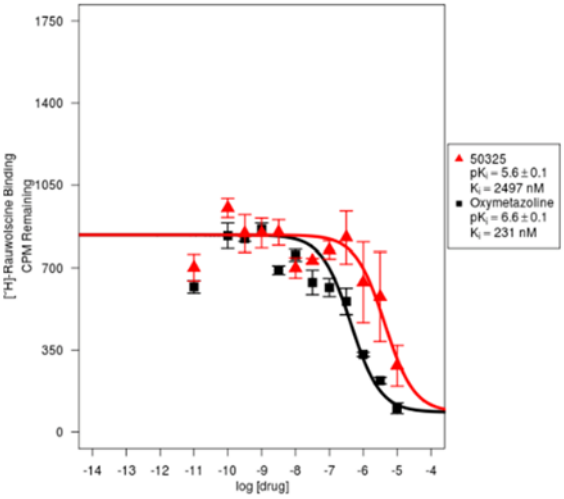

DOR binding of **25** MRS4525 (PDSP 50325)

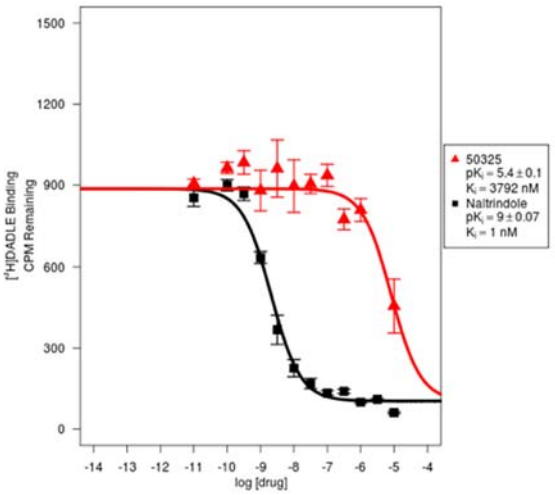

σ_1 binding of **25** MRS4525 (PDSP 50325)

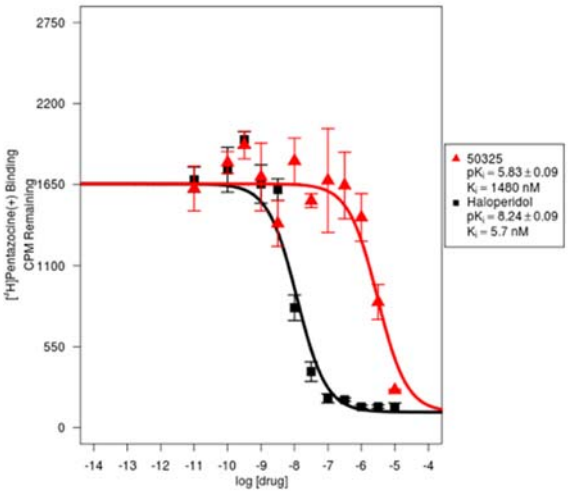

σ_2 binding of **25** MRS4525 (PDSP 50325)

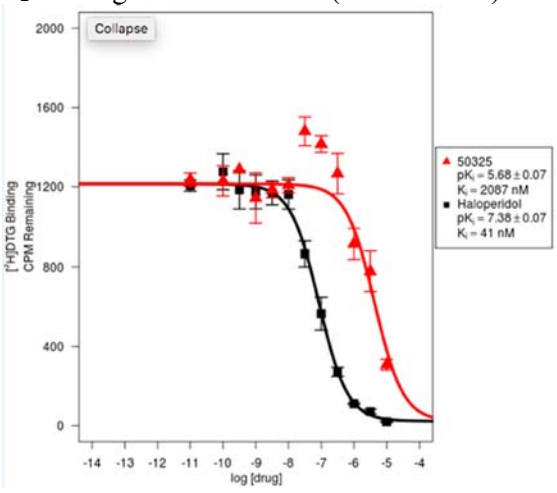

DOR binding of **26** MRS4526 (PDSP 50326)

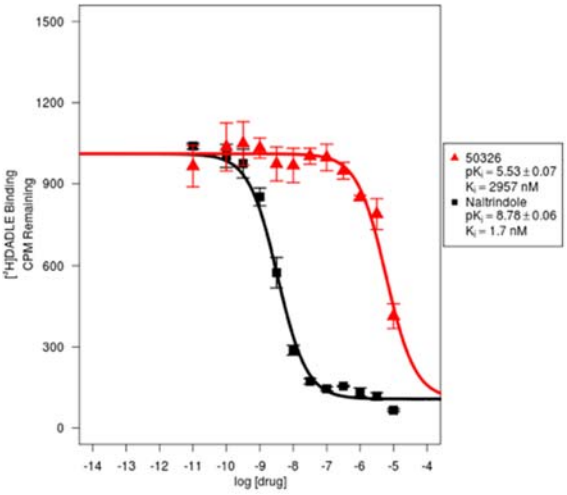

σ_1 binding of **26** MRS4526 (PDSP 50326)

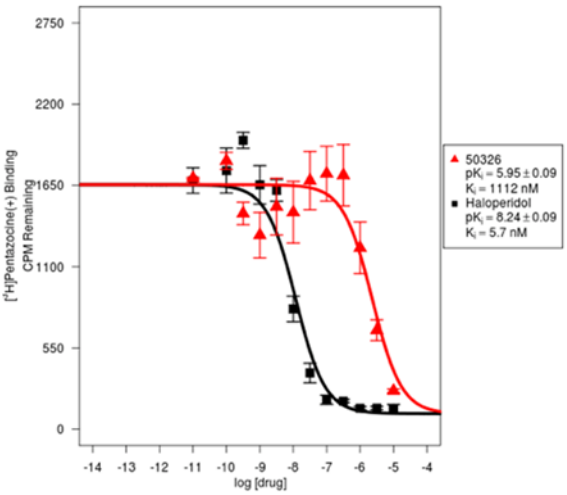

σ_2 binding of **26** MRS4526 (PDSP 50326)

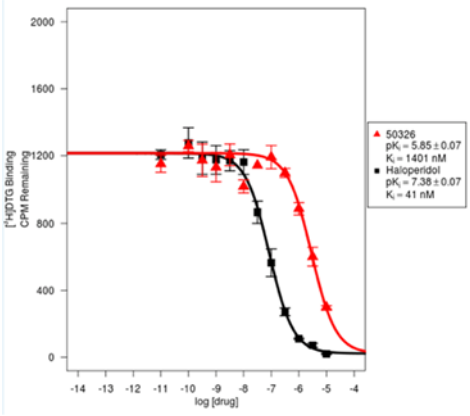

Synthesis and analysis of [^{3}H]PPTN 1 (5 mCi)

Synthetic procedure (refer to Scheme 5):

A, JYH-029 (**39**, 6 mg, 10 μmol) was combined with Pd/C (10% on charcoal, 5 mg) in ethyl acetate (0.2 mL). The reaction mixture was evacuated, and tritium gas was added. The mixture stirred for 24 h at room temperature. The reaction mixture was filtered through Acrodisc Syringe Filters, and the filtrate was evaporated with methanol 3 times and the compound **93** obtained subjected to assay.

B, **94**, [^{3}H]JYH-031 (**93**) was dissolved in 1 mL of THF, and 0.1 mL of TFA was added slowly and the mixture stirred for 4 h at room temperature. The reaction mixture was evaporated to dryness.

C, [^{3}H]**1**, [^{3}H]JYH-014 (**94**) was slowly dissolved in 1 mL of water:methanol (1:1, by volume), and 0.1 mL 1N KOH was added slowly and the mixture stirred for 18 h at room temperature. The reaction mixture was evaporated to dryness.

D, Purification of [^{3}H]**1**:

The residue from the last step was purified on an HPLC-C18 column, with a mobile phase gradient (A: 0.1% aqueous TFA, B: 100% acetonitrile) of 100% A to 100% B in 60 min, and flow rate of 6 mL/min, UV detection at 268 nm. The isolated material was demonstrated to be homogeneous in a radiochemical/HPLC assay.

E, **Figure S3**. Quality control of [^{3}H]**1**: HPLC Data Set:

A

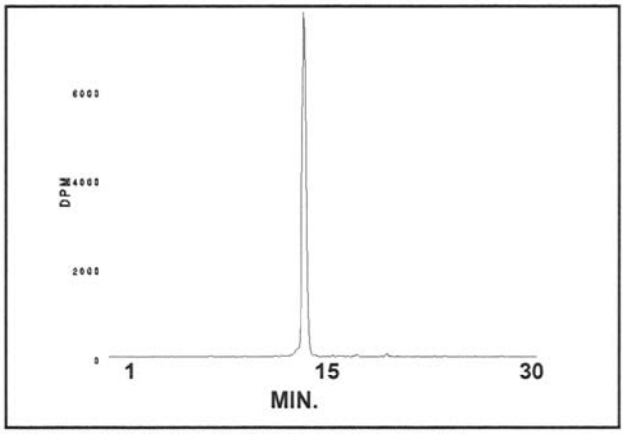

HPLC ANALYSIS LOT 591-041-0211-A-20180620-JPL
File Name: int4g06l Date and Time: 6/21/2018 8:08:13 PM
Unit 04 Radio

Peak #	Area %	Time	Area
1	2.00	13.23000	308.90447
2	97.03	13.67000	15010.27087
3	0.12	14.48000	17.98099
4	0.15	15.75670	23.71037
5	0.34	17.45000	52.21468
6	0.37	19.50670	56.84149
Totals	100.00		15469.92287

Specific Activity: 21.1 Ci/mmol

Concentration: 1.0 mCi/ml; 24.55 µg/ml

Packaged in: Ethanol solution

Date of Analysis: June 21, 2018

Radiochemical Purity: 97.0%

Column: Symmetry Shield RP18 4.6 x 150mm, 3.5µm

Flow Rate: 1 ml/min.

Mobile Phase: A: 0.1% TFA in water
B: Acetonitrile
0-20min 0%-100% B;
Hold to 30min

B

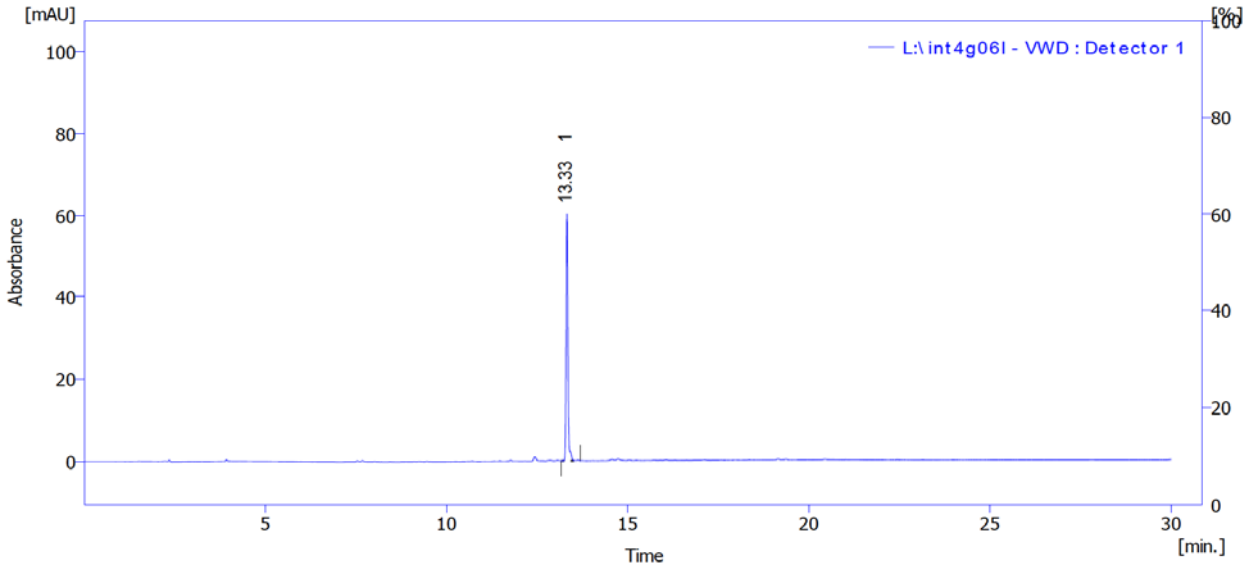

C

MS Data Set

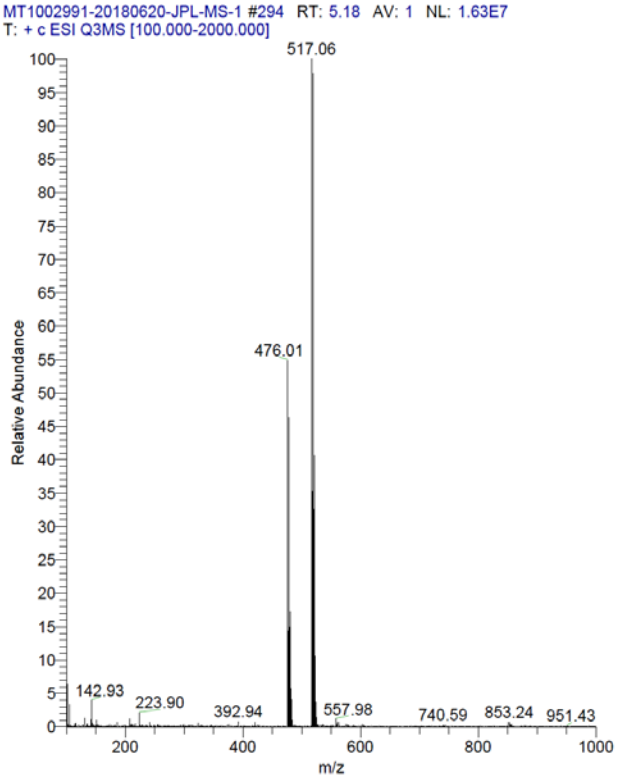

Behavior of [^{3}H]PPTN in solution and in interaction with cell membranes

[^{3}H]PPTN was either precipitating or adhering to vessels during storage of the ethanol source solution and its aqueous dilution. We tried warming but there was no liberation of PPTN from the walls of the vessel. We compared the solubility of unlabeled PPTN (HCl salt from Tocris), we compared a 100-fold dissolution from 5 mM DMSO stock into either pure EtOH, pure water, or a 1:1 mixture of EtOH and water. All three showed no visible signs of precipitation.

Aqueous [^{3}H]PPTN tended to stick to plastic surfaces (very efficiently, within minutes, **Figure S4** below), but not glass surfaces. See the plot below, in which aliquots were counted over time post-dilution from the EtOH stock and comparing keeping the diluted solution at room temperature in either glass and polypropylene tubes. The initial concentration in the aqueous medium (PBS) was 10 nM, diluted by 1000-fold from the 10 µM source solution.

Figure S4.

A

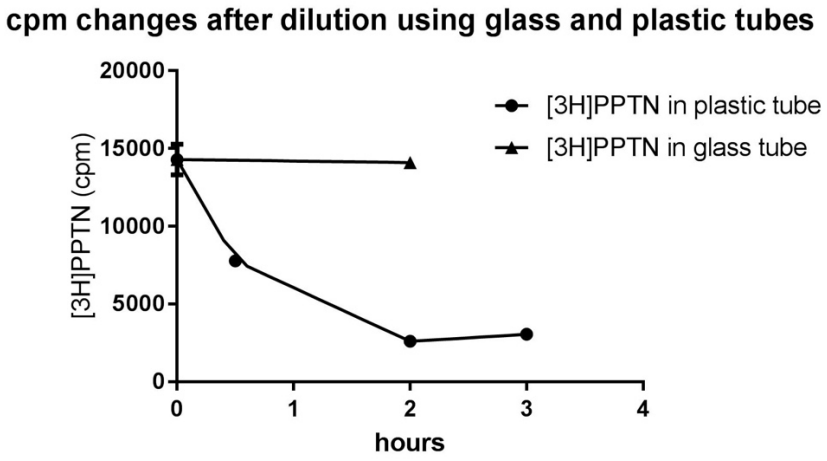

We compared the specific and non-specific binding of [^{3}H]PPTN **1** to membranes of $P2Y_{14}$ receptor-expressing CHO cells, using our standard incubation protocol for GPCRs in general. The level of nonspecific binding was unacceptably high for reliable results (estimated at >90% of the total radioactivity, figure below), even when the glass fiber filters used to separate bound from unbound label were pretreated with polyethyleneimine (a technique we have used successfully in some other difficult cases). We conclude that the radioligand, unfortunately, will not be useful for us to screen new drug compounds, at least using membrane preparations.

B

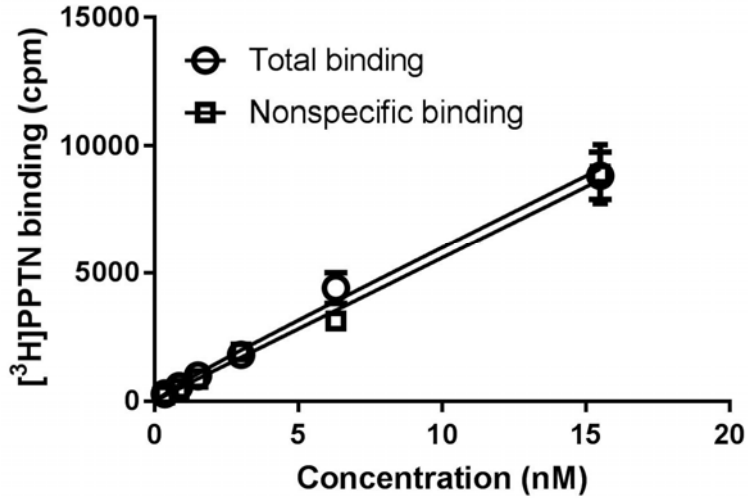

Figure S5. Correlation plot of cLogP vs. pIC_{50}

Numbers refer to compounds listed in Table 1

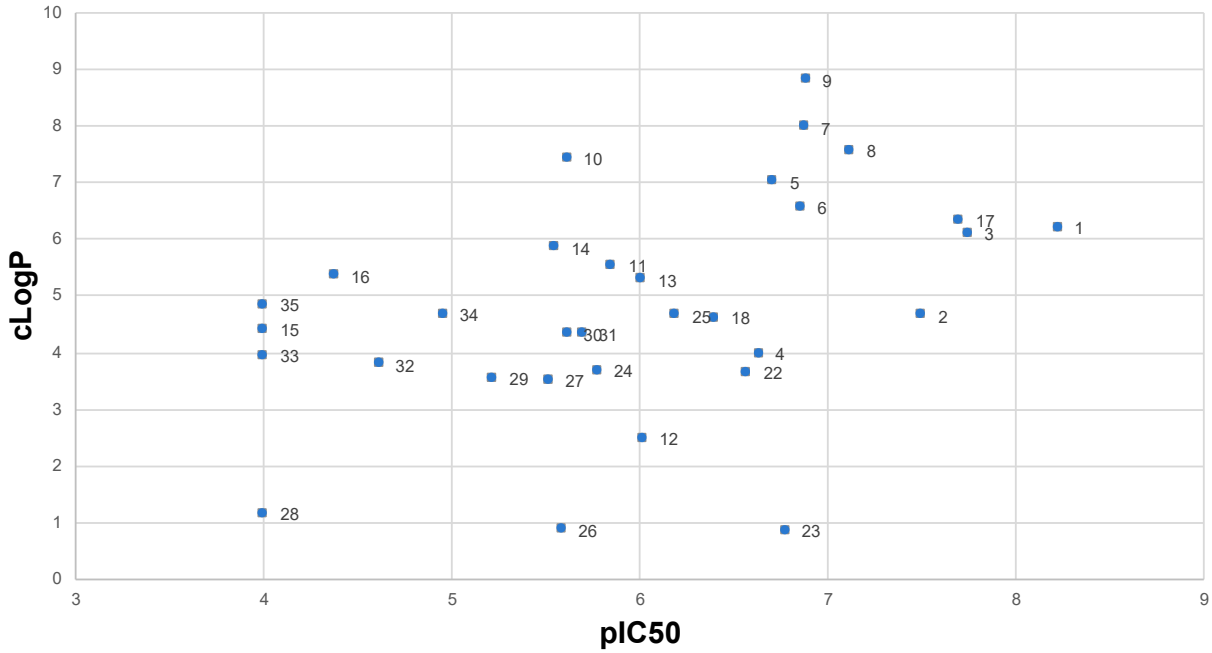

Table S1. Comparison of functional (forskolin-stimulated cAMP inhibition)[a] and fluorescent binding data at the human $P2Y_{14}$ receptor.

Average ratio (fluorescent binding IC_{50} / cAMP IC_{50}) = 17.8 ± 6.3 (mean ± SEM)

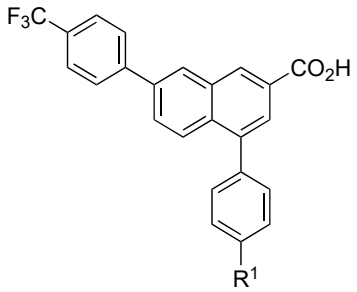

Compound	R^1 = , other changes	cAMP IC_{50} (nM)[a]	Fluorescent binding IC_{50} (nM)[b]	ratio
1[b] PPTN	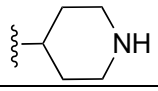	0.3±0.1	6.0±0.1	20.0
5 MRS4576 (cf. 4179)	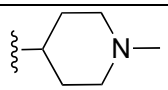	7.1±1.6	195±120	27.5
8 MRS4149	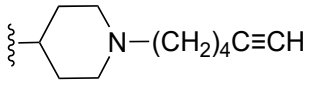	13.0±1.1	76.3±24.4	5.87

a. Kiselev, E., Barrett, M., Katritch, V., Paoletta, S., Weitzer, C.D., Hammes, E., Yin, A.L., Zhao, Q., Stevens, R.C., Harden, T.K., Jacobson, K.A. Exploring a 2-naphthoic acid template for the structure-based design of $P2Y_{14}$ receptor antagonist molecular probes. ACS Chem. Biol., 2014, 9: 2833-2842.

b. This study (Table 1A).

ADME-tox parameters (determined by Jai Research Foundation (JRF), Department of Toxicology, Valvada - 396 105, Dist. Valsad, Gujarat, India): Protocol RES 1-04-23610 (MRS4608) and RES 1-04-23609 (MRS4619)

Table S2. HepG2 cell (hepatocyte) cytotoxicity for MRS4608 and MRS4619

Test Compound	IC_{50} (μM)
17, MRS4608	21.62
18, MRS4619	cells are 100% viable at highest tested (30 μM) concentration
Verapamil	55.02

Figure S6. Mean plasma concentration of **17**, MRS4608 and **18**, MRS4619 in Wistar rats after i.v. or i.p. administration.
Vehicle: i.v.; i.p.

A

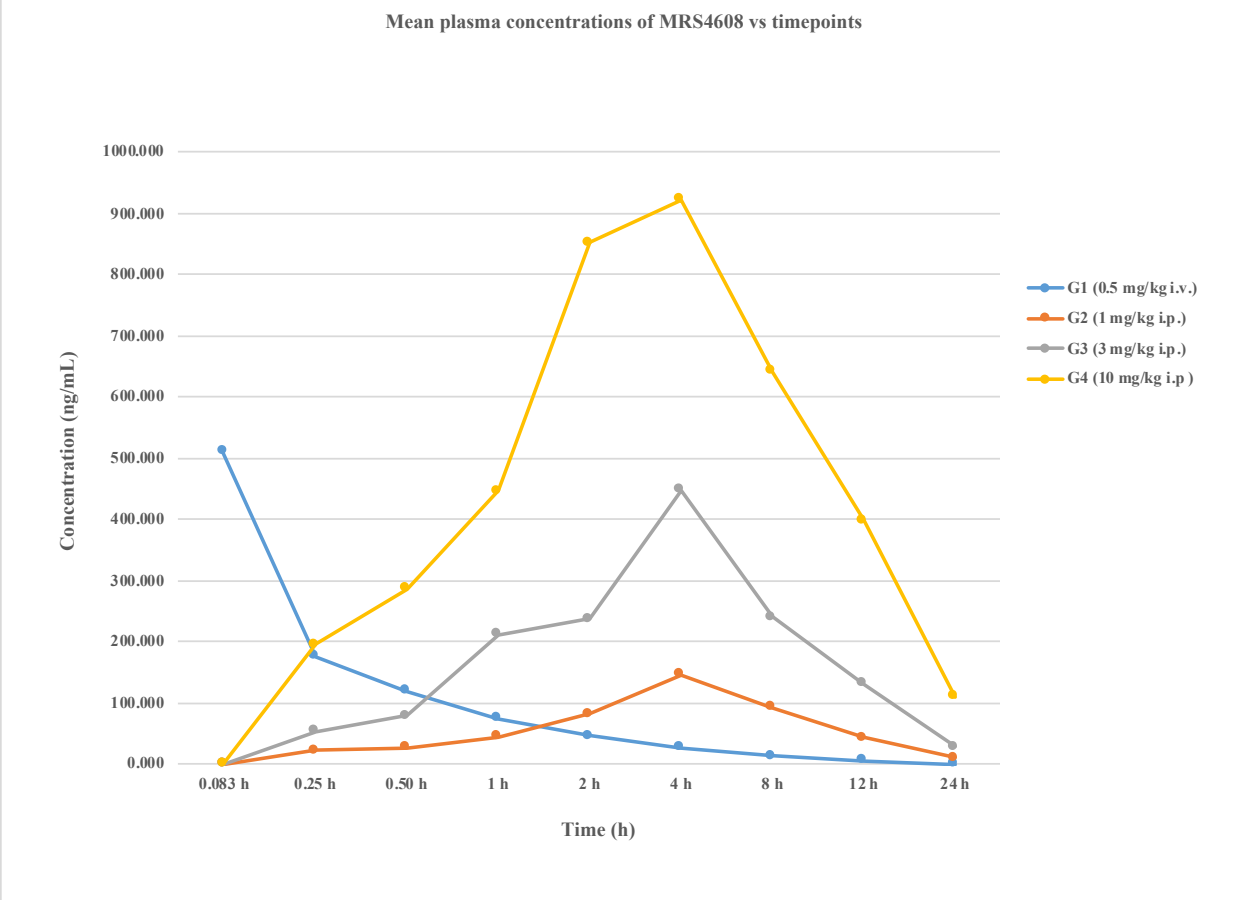

B

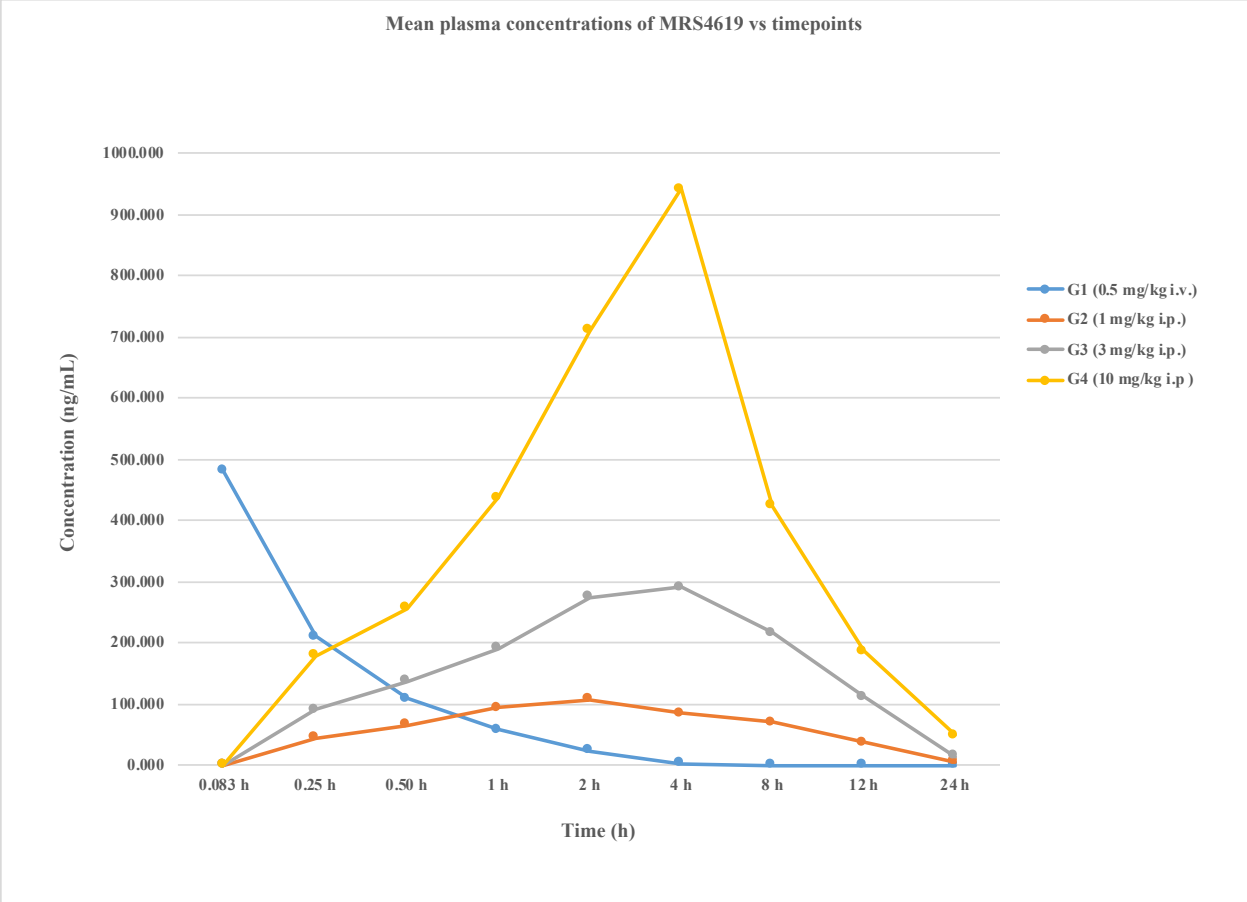
Mean plasma concentrations of MRS4619 vs timepoints
Concentration (ng/mL)
1000.000
900.000
800.000
700.000
600.000
500.000
400.000
300.000
200.000
100.000
0.000
0.083 h
0.25 h
0.50 h
1 h
2 h
4 h
8 h
12 h
24 h
Time (h)
G1 (0.5 mg/kg i.v.)
G2 (1 mg/kg i.p.)
G3 (3 mg/kg i.p.)
G4 (10 mg/kg i.p)

Table S3. Single dose pharmacokinetic parameters for **17**, MRS4608 (A) and **18**, MRS4619 (B) through intravenous and oral routes in Wistar Rats.

A

Group (Dose, mg/kg)	C_{max} (ng/mL)	T_{max} (h)	AUC_{0-last} (h* ng/mL)	$AUC_{0-\infty}$ (h*ng/mL)	$T_{1/2}$ (h)	MRT_{last} (h)	Vd (mL/kg)	Kel (1/h)	F (%)	Cl (mL/h/kg)
i.v. (0.5)	511.2	0.083	450.9	479.9	3.460	2.486	5201	0.200	100.0	1042
i.p. (1.0)	146.6	4.000	1388	1461	5.114	7.625	5051	0.136	153.9	684.6
i.p. (3.0)	447.5	4.000	4080	4295	5.246	7.506	5286	0.132	150.8	698.5
i.p. (10)	923.1	4.000	10960	11960	6.325	8.092	7630	0.110	121.4	836.2

B

Group (Dose Levels)	C_{max} (ng/mL)	T_{max} (h)	AUC_{0-last} (h* ng/mL)	$AUC_{0-\infty}$ (h*ng/mL)	$T_{1/2}$ (h)	MRT_{last} (h)	Vd (mL/kg)	Kel (1/h)	F (%)	Cl (mL/h/kg)
i.v. (0.5)	482.5	0.083	256.7	260.1	0.720	0.634	1998	0.962	100.000	1923
i.p. (1.0)	106.7	2	1137	1178	4.612	7.162	5646	0.150	221.401	848.6
i.p. (3.0)	291.3	4	3352	3445	4.192	7.256	5267	0.165	217.7	870.8
i.p. (10)	943.1	4	7848	8223	5.335	6.671	9361	0.130	152.9	1216

Molecular modeling

Table S4. Summary of the MD trajectories analysis (5 replicates) of the complex between hP2Y$_{14}$R and compounds **17**. The average root mean square deviation of the ligand heavy atoms relative to the docking pose ($RMSD_{ave}$), after alignment of the protein Cα atoms to the starting structure; the average ligand-receptor electrostatic (Ele), van der Waals (vdW) and sum of the two (Total) interaction energy (En_{ave}) are indicated. The percentages of frames showing hydrogen bonds between the ligand and Lys77$^{2.60}$, Tyr102$^{3.33}$, Lys277$^{7.35}$ are reported. The replicates discussed in the manuscript (selected on the basis of the lowest average ligand RMSD) are highlighted in red.

Replicates		**1**	**2**	**3**	**4**	**5**
$RMSD_{ave}$ (Å)		3.27	3.45	2.22	2.97	3.35
Inter-rep $RMSD_{ave}$ (Å)		3.05				
En_{ave} (kcal/mol)	**Ele**	-157.28	-134.82	-152.58	-145.32	-179.15
	Inter-rep Ele	-153.83				
	vdW	-32.14	-37.27	-31.97	-36.14	-29.96
	Inter-rep vdW	-33.50				
	Total	-189.42	-172.09	-184.55	-181.46	-209.11
	Inter-rep Tot	-187.33				
Hydrogen Bonds	**Lys77$^{2.60}$**	74%	22%	91%	20%	17%
	Tyr102$^{3.33}$	22%	3%	7%	56%	13%
	Lys277$^{7.35}$	70%	25%	87%	71%	80%

Figure S7.

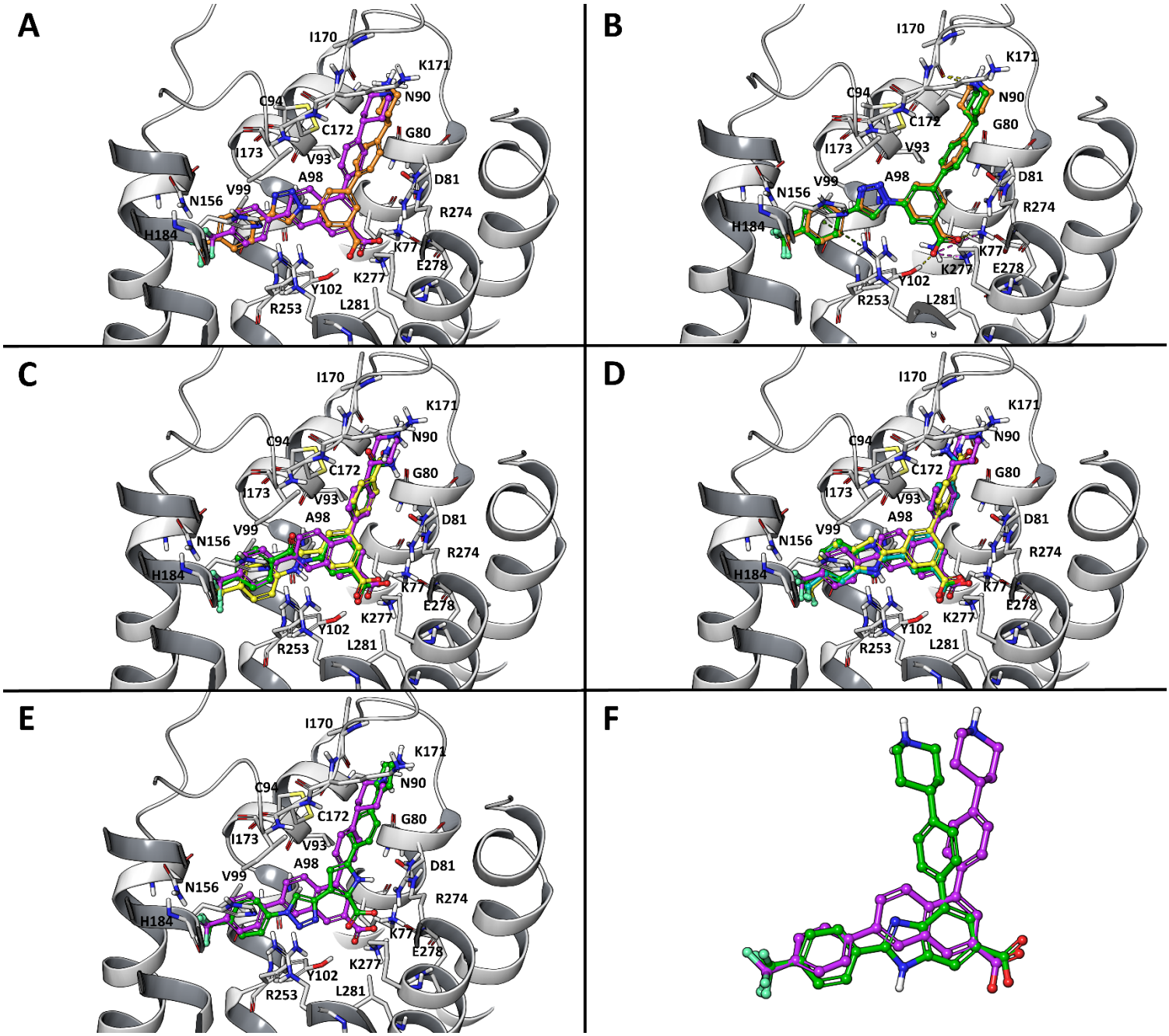

Figure S7. Docking poses of **A)** compounds **1** (PPTN) (purple) and **2** (orange); **B)** compounds **15** (green) and **2** (orange) as reference; **C)** compounds **27** (green), **29** (yellow) and **1** (purple) as reference; **D)** compounds **30** (green), **31** (yellow), **32** (cyan) and **1** (purple) as reference; **E)** compounds **33** (green) and **1** (purple) as reference, at hP2Y$_{14}$R. The receptor is represented in light gray. Panel **F)** shows the superposition of compound **35** to compound **1**, using as constraints the carboxylic carbon atom, the trifluoromethyl carbon atom, and the attachment point of the piperidine-phenyl group.

Figure S8.

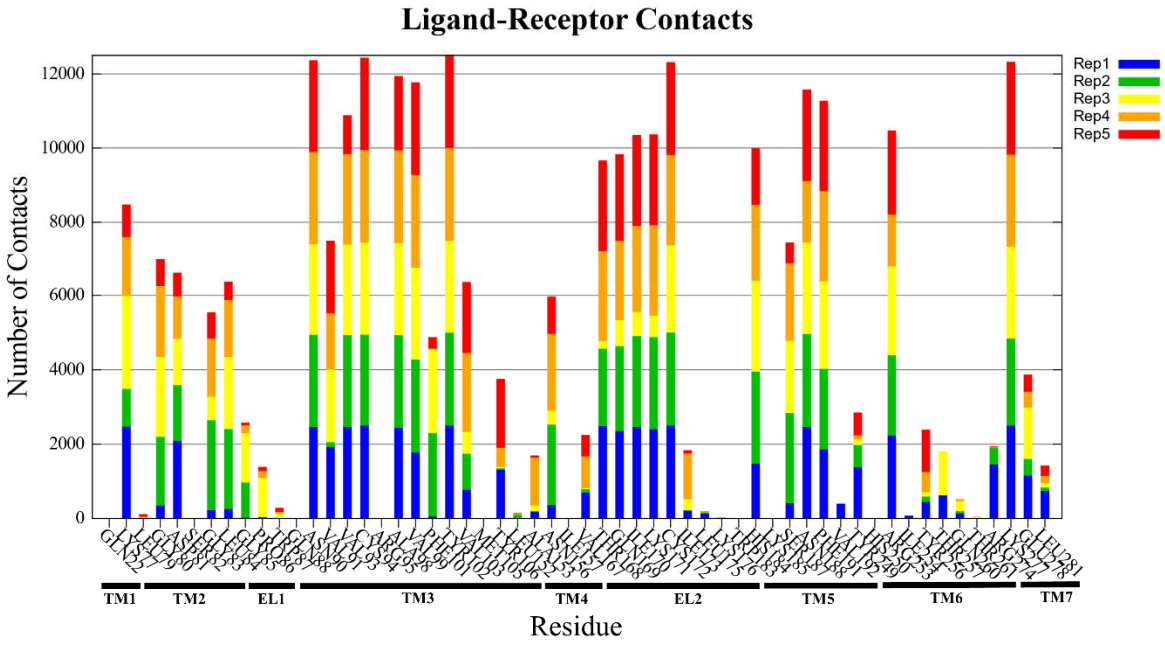

Figure S8. Number of contacts (distance within 4 Å) between the compound **17** and the hP2Y$_{14}$R's residues during the simulations. Residues with no contacts with the ligand in none of the simulations are not reported. The results for replicates 1, 2, 3, 4 and 5 are showed in blue, green, yellow, orange and red, respectively. The simulations (50 ns) were saved with a stride of 20 ps, resulting in 2500 frames (maximum number of contacts during a replicate). A bar at the bottom of the histograms shows the topological region of each residue.

Figure S9.

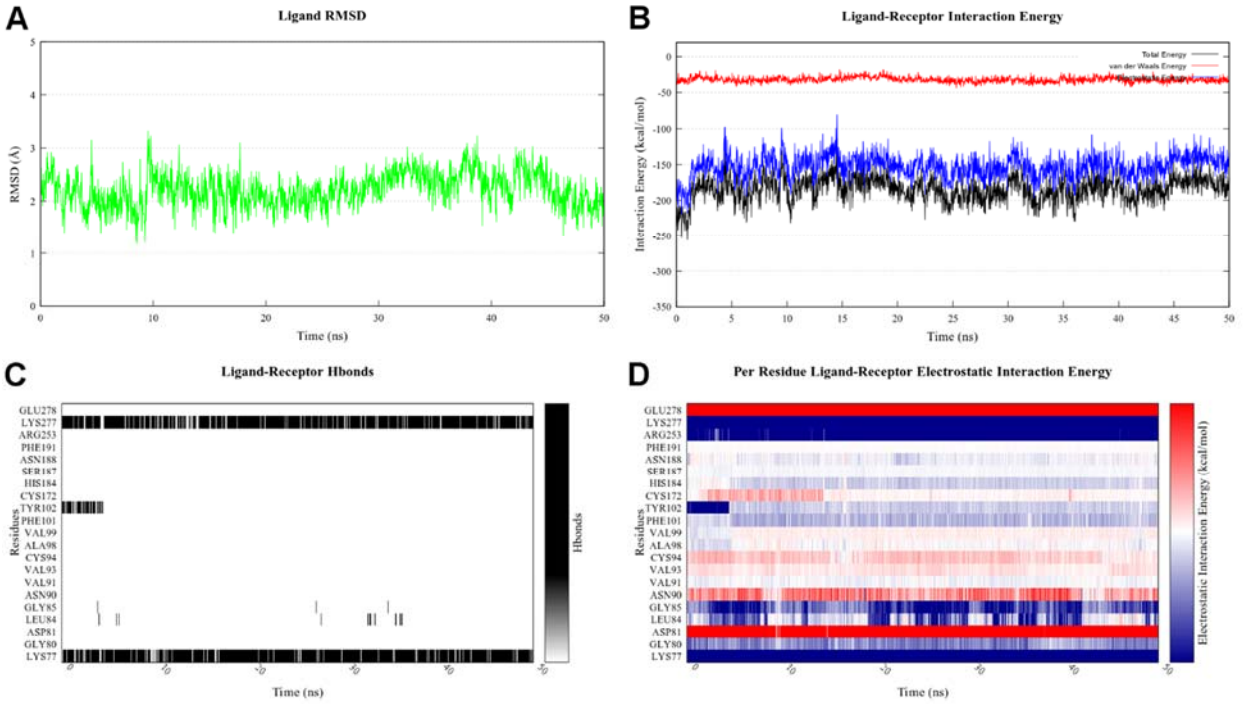

Figure S9. Analysis of the MD simulation (replicate 3) of the complex between compound **17** and hP2Y$_{14}$R. The replicate was chosen considering the lowest average ligand RMSD. **A)** RMSD of ligand heavy atoms relative to the docking pose, after alignment of the protein Cα atoms to the initial structure. **B)** Electrostatic and van der Waals (and Total, as sum of the two) ligand-receptor interaction energy. **C)** Hydrogen bonds between the ligand and residues that are in contact (within 4 Å) with it for at least half of the simulation. **D)** Electrostatic interaction between the ligand and residues that are in contact (within 4 Å) with it for at least half of the simulation. A colorimetric scale going from blue to red indicates negative to positive energy values.

Figure S10.

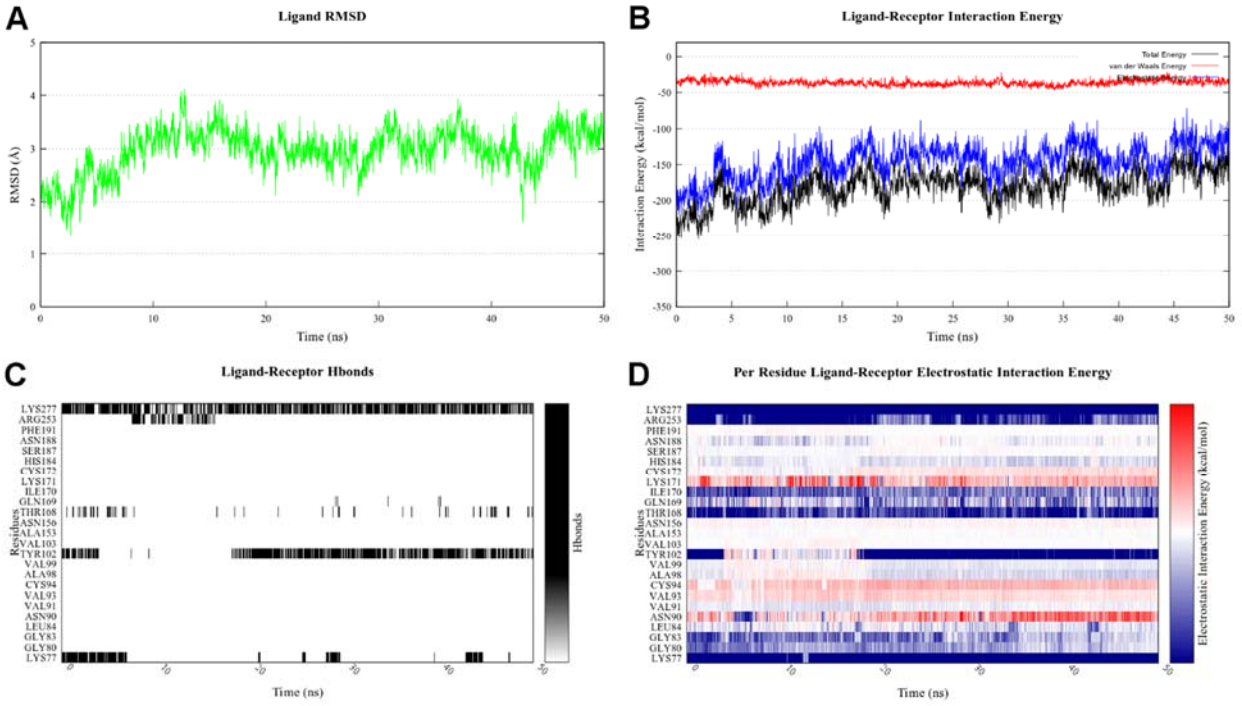

Figure S10. Analysis of the MD simulation (replicate 4) of the complex between compound **17** and hP2Y$_{14}$R. The replicate was chosen considering the lowest average ligand RMSD. **A)** RMSD of ligand heavy atoms relative to the docking pose, after alignment of the protein Cα atoms to the initial structure. **B)** Electrostatic and van der Waals (and Total, as sum of the two) ligand-receptor interaction energy. **C)** Hydrogen bonds between the ligand and residues that are in contact (within 4 Å) with it for at least half of the simulation. **D)** Electrostatic interaction between the ligand and residues that are in contact (within 4 Å) with it for at least half of the simulation. A colorimetric scale going from blue to red indicates negative to positive energy values.

Video S1. MD trajectory (replicate 3) of the complex between compound **17** and hP2Y$_{14}$R, after alignment of the receptor Cα atoms to the initial frame. The receptor is depicted by a grey ribbon and the ligand by green sticks. The tips of TM6 and TM7 are transparent to enable the visualization of the ligand. Residues in contact with the ligand (within 4 Å) for at least half of the simulation are highlighted by sticks. Hydrogen bonds are shown by dashed lines. Water molecules around 2.5 Å from the ligand are rendered by red spheres.

Video S2. MD trajectory (replicate 4) of the complex between compound **17** and hP2Y$_{14}$R, after alignment of the receptor Cα atoms to the initial frame. The receptor is depicted by a grey ribbon and the ligand by green sticks. The tips of TM6 and TM7 are transparent to enable the visualization of the ligand. Residues in contact with the ligand (within 4 Å) for at least half of the simulation are highlighted by sticks. Hydrogen bonds are shown by dashed lines. Water molecules around 2.5 Å from the ligand are rendered by red spheres.

Procedures for measuring pION solubility and lipophilicity

Solubility using a modified pION method,[1,2] and lipophilicity was measured based on the HPLC retention time.[3]

pION solubility tests. *pION buffer and blank buffer preparation.* pION solubility tests were performed with pION system solution (pION, Inc., Billerica, MA, USA, P/N 110151). pH 4.0 and 7.4 pION buffers were prepared by adding 2.5 mL of pION system solution to 97.5 mL of Milli Q water and adjusting the pH to 4.0 and 7.4 with 0.5 N NaOH, respectively. Blank buffers were prepared by mixing 15 mL of pION buffers (pH 4.0 and 7.4) with 14 mL of *n*-propanol.

Control and sample UV plate preparation. All ligands were stored as 5 mM stock solutions in dimethyl sulfoxide (DMSO). 3 µL of each ligand stock solution (including DMSO control) was added to 300 µL of pH 4.0 and 7.4 pION buffers, mixed and incubated for 20 hours. The undissolved compound particles were removed by centrifuge at 14,000 rpm for 20 min. 100 µL of supernatant was added to a 96 well plate containing 100 µL of *n*-propanol and mixed well with pipette.

Reference UV plate preparation. 4 µL of each ligand stock solution was added to 76 µL of *n*-propanol. 10 µL of resulting solution was added to 290 µL of blank buffer, mixed and incubated for 20 hours. 200 µL of the reference solution with final concentration of ligand as 8.33 µM was transferred to a 96 well plate.

UV absorption tests. The Greiner UV-Star® 96 well plates have low UV absorption background and excellent resistance to general organic solvents. The UV absorption of control ($A_{control}$), ligands (A_{ligand}), and references ($A_{reference}$) were collected in triplicate at the ligands' maximum absorption at 270 nm.

Solubility calculation. $Solubility_{(ligand)}$ = 2 x average (A_{sample}-$A_{control}$)/average ($A_{reference}$-$A_{control}$) x 8.33 µM = 2 x average (A_{sample}-$A_{control}$)/average ($A_{reference}$-$A_{control}$) x 8.33 x M_w x 10^{-3} µg/mL.

Relative lipophilicities of PPTN analogues compared to compound 1. All ligands were stored as 250 µM stock solutions in dimethyl sulfoxide (DMSO). HPLC based measurements of relative lipophilicities of analogues of **1** compared to **1** were carried out with an Agilent Eclipse XDB-C18 (5 µm) and a 20 min gradient of 10% to 100% acetonitrile in 10 mM triethylammonium acetate. The relative lipophilicity of **1** analogues compared to **1** was indicated by the retention factor difference between ligands and **1** ($\Delta k = k_{analogues} - k_1$; $k = (t_R - t_0)/t_0$).

1. Kiselyuk, A. S. *HNF4 alpha bioactive ligands discovered by a high- throughput screen for modulators of the human insulin promoter.* (Doctoral dissertation, pp. 65). University of California, San Diego, 2011. (https://escholarship.org/content/qt64k4q3gr/qt64k4q3gr.pdf)

2. Yan, Z.; Caldwell, G. *Optimization in Drug Discovery: In Vitro Methods* (pp. 58). Humana Press.

3. Valkó, K.; Application of high-performance liquid chromatography based measurements of lipophilicity to model biological distribution. *J. Chromatogr. A* **2004,** *1037*, 299–310.